Cancer Cell
Article

p53-Mediated Senescence Impairs the Apoptotic Response to Chemotherapy and Clinical Outcome in Breast Cancer

James G. Jackson,[1] Vinod Pant,[1] Qin Li,[1,5] Leslie L. Chang,[1] Alfonso Quintás-Cardama,[2] Daniel Garza,[1] Omid Tavana,[3] Peirong Yang,[1] Taghi Manshouri,[2] Yi Li,[6] Adel K. El-Naggar,[4] and Guillermina Lozano[1,*]
[1]Department of Genetics
[2]Department of Leukemia
[3]Department of Immunology
[4]Department of Pathology
The University of Texas MD Anderson Cancer Center, Houston, TX 77030, USA
[5]The University of Texas Graduate School of Biomedical Sciences Program in Genes and Development, Houston, TX 77030, USA
[6]Lester & Sue Smith Breast Center and Department of Molecular and Cell Biology, Baylor College of Medicine, Houston, TX 77030, USA
*Correspondence: gglozano@mdanderson.org
DOI 10.1016/j.ccr.2012.04.027

SUMMARY

Studies on the role of *TP53* mutation in breast cancer response to chemotherapy are conflicting. Here, we show that, contrary to dogma, MMTV-*Wnt1* mammary tumors with *mutant* p53 exhibited a superior clinical response compared to tumors with wild-type p53. Doxorubicin-treated *p53* mutant tumors failed to arrest proliferation, leading to abnormal mitoses and cell death, whereas *p53* wild-type tumors arrested, avoiding mitotic catastrophe. Senescent tumor cells persisted, secreting senescence-associated cytokines exhibiting autocrine/paracrine activity and mitogenic potential. Wild-type p53 still mediated arrest and inhibited drug response even in the context of heterozygous *p53* point mutations or absence of p21. Thus, we show that wild-type *p53* activity hinders chemotherapy response and demonstrate the need to reassess the paradigm for *p53* in cancer therapy.

INTRODUCTION

The tumor suppressor *TP53* is mutated or inactivated in the majority of cancers (Soussi and Lozano, 2005). *p53* exerts its effects by binding specific promoter sequences following cellular stress and activating transcription of genes involved in cell-cycle arrest, senescence, and apoptosis (Riley et al., 2008). DNA damage, such as that induced by radiation or chemotherapy drugs, is a potent activator of p53.

Classic studies using mouse models have demonstrated an in vivo role for *p53* in the induction of apoptosis following DNA damage (Jackson et al., 2011). Thymocytes from *p53* null mice do not undergo apoptosis after radiation (Clarke et al., 1993; Lowe et al., 1993b), and the embryonic neural tube in *p53* null mice is similarly resistant (Lang et al., 2004; Liu et al., 2004). *p53* also contributes to response after exposure to DNA-damaging drugs by inducing apoptosis in E1A/Ras-transformed mouse embryo fibroblasts (Lowe et al., 1993a, 1994).

Interestingly, studies examining the paradigm that wild-type *p53* activity improves drug response are lacking in tumors arising from epithelial tissues (Brown and Attardi, 2005). This deficiency is exemplified in breast cancer. Some reports on the response of breast cancer with or without *TP53* mutation to chemotherapy drugs have been inconclusive (Bonnefoi et al., 2011; Makris et al., 1995; Mathieu et al., 1995), whereas others show that wild-type *TP53* activity is beneficial to response (Aas et al., 1996; Berns et al., 2000; Kröger et al., 2006; Rahko et al., 2003). Intriguingly, still other reports have shown that *TP53*

Significance

Approximately one-third of human breast cancers harbor mutations in the tumor suppressor gene *TP53*. The long-held paradigm that wild-type p53 mediates apoptosis resulting in a favorable chemotherapy response is less clear in breast cancer because many reports conflict, including some suggesting that tumors harboring *TP53* mutations respond more favorably. Here, we show that wild-type p53 activity is paradoxically detrimental to chemotherapy response because, unlike mutant *p53* tumors, *p53* wild-type tumors can avoid aberrant mitoses by undergoing arrest, which is followed by expression of cytokines in senescent cells that can stimulate cell proliferation and tumor relapse. Furthermore, our data demonstrate that in order to accurately predict clinical response of *TP53*-mutated tumors, the status of the second allele must be determined.

mutant tumors respond better (Bertheau et al., 2002, 2007; Mathieu et al., 1995). It is unclear why these reports reached different conclusions, and importantly, the notion that wild-type *TP53* activity would hinder response, given its known apoptotic and tumor suppressive functions, is controversial and lacks a mechanistic explanation. Thus, it is desirable to have a controlled setting to examine if wild-type p53 activity is beneficial in breast cancer response, and if not, as some have suggested (Bertheau et al., 2008), then why?

RESULTS

Superior Response of *p53* Mutant Mammary Tumors to Doxorubicin Treatment

In order to address the role of the *p53* response in breast cancer, we bred MMTV-*Wnt1* (Tsukamoto et al., 1988) mice into *p53* wild-type as well as $p53^{-/-}$ (Jacks et al., 1994) and $p53^{R172H}$ (Lang et al., 2004) ("*p53* mutant" herein) backgrounds. p53R172H is a structurally defective mutant that cannot bind DNA, and mice that are homozygous or heterozygous for this mutation are identical to $p53^{-/-}$ or $p53^{+/-}$ mice, respectively, in survival (Lang et al., 2004) and for results presented here. After mammary tumors formed, mice were treated with doxorubicin and monitored. We found that, despite heterogeneity of responses (see Figure S1A available online), tumors from mice in the wild-type *p53* background generally underwent minimal tumor regression, stabilized for several days, and quickly relapsed (Figures 1A and 1E).

We next examined *p53* mutant MMTV-*Wnt1* mammary tumors. In most human tumors, biallelic point mutations or deletions of *p53* are relatively rare. More typically, a *p53* point mutation is acquired in a single allele, and the other allele is subsequently retained or lost. Thus, we treated MMTV-*Wnt1* *p53* heterozygous mutant mice ($p53^{R172H/+}$ genotype) bearing tumors, of which approximately 40% undergo loss of heterozygosity (LOH) for the wild-type *p53* allele (Donehower et al., 1995). Surprisingly, we found that tumors in $p53^{R172H/+}$ MMTV-*Wnt1* mice that lost the wild-type allele (rendering the tumor $p53^{R172H/0}$ and functionally null) showed greater tumor regression and longer time to relapse (Figures 1B, 1E, and S1B).

Also to our surprise, we found that as long as tumors from $p53^{R172H/+}$ mice retained the wild-type *p53* allele, they exhibited a response typical of *p53* wild-type tumors (Figures 1C and S1C), despite the presence of a mutant allele with reported dominant-negative activity (Lang et al., 2004; Willis et al., 2004). We also observed dramatic tumor volume reductions in MMTV-*Wnt1* mammary tumors from treated *p53* homozygous mutant mice (Figures 1D and S1D), although these mice were typically harvested within 1 week following the final doxorubicin treatment (Figure 1D) due to gastrointestinal syndrome (Komarova et al., 2004). Use of the *p53* homozygous mutant mice was also limited by the difficulty of acquiring females in the cohort (Sah et al., 1995). In sum although tumors of all genotypes eventually relapsed, treated tumors lacking all p53 activity, whether homozygous null or heterozygous mutant with LOH, had significantly greater decrease in tumor volume and significantly longer time to relapse compared to tumors retaining p53 activity (Figure 1E).

To assess the acute biochemical response to treatment, we examined *p53* function in MMTV-*Wnt1* tumors 24 hr after the final doxorubicin dose. *p53* target genes *p21*, *Puma*, and *Ccng1* were induced 4- to 6-fold compared to untreated tumors (Figure 1F), demonstrating retention of wild-type *p53* in MMTV-*Wnt1* tumors from $p53^{+/+}$ mice, as others have shown (Donehower et al., 1995). Predictably, *p53* homozygous mutant tumors did not induce target genes (Figure 1F). *Noxa* levels, however, were elevated in some tumors in a *p53*-independent fashion. *p53* heterozygous mutant MMTV-*Wnt1* tumors that retained the wild-type allele also induced *p53* target genes, in contrast to tumors with *p53* LOH (Figure 1G).

To address the mechanism of response in *p53* wild-type versus mutant tumors, we examined growth arrest and apoptosis in tumors 24 hr after doxorubicin treatment. Examining proliferation, we found that untreated tumors of all genotypes were highly positive for Ki67, a marker of cells outside G0 of the cell cycle. Following treatment, only *p53* wild-type MMTV-*Wnt1* tumors had large areas that were Ki67 negative or sparsely positive, demonstrating cell-cycle exit, whereas *p53* mutant tumors remained positive for Ki67 (Figure 2A). Furthermore, tumors from parallel orthotopic transplants of a *p53* wild-type MMTV-*Wnt1* tumor ceased incorporating bromodeoxyuridine (BrdU) following treatment, whereas transplanted *p53* mutant tumors continued to enter S phase (Figure 2B). This failure to arrest in the presence of DNA damage resulted in aberrant mitoses, as evidenced by anaphase bridges, in treated *p53* mutant tumors, whereas *p53* wild-type tumors arrested and, thus, were not mitotic (Figures 2C–2E). The *p53* mutant MMTV-*Wnt1* tumors also showed a significant increase in both cleaved caspase-3 and terminal deoxynucleotidyl transferase dUTP nick end labeling (TUNEL)-positive cells after doxorubicin treatment (Figure 2F). *p53* wild-type tumors, however, did not undergo apoptosis following treatment (Figure 2F). Taken together, our data show that despite induction of apoptotic genes such as *Puma* and *Noxa*, growth arrest, not apoptosis, was acutely induced in *p53* wild-type tumors following doxorubicin treatment, and lack of arrest in mutant tumors resulted in aberrant mitoses, cell death, and ultimately, a superior clinical response.

Doxorubicin Induces a Senescent-like Phenotype in *p53* Wild-type Mammary Tumors

To further address the mechanism responsible for the suboptimal response in *p53* wild-type tumors, we harvested *p53* wild-type or heterozygous MMTV-*Wnt1* tumors 5–7 days post-treatment (Figures S2A–S2C) and examined them for markers of senescence. We quantitatively determined that many markers of senescence (*p21*, *Dcr2*, *p16*, *p15*, *Dec1*, and *Pml*) (Collado et al., 2005; te Poele et al., 2002) were elevated in many stably arrested MMTV-*Wnt1* tumors that were *p53* wild-type or heterozygous with retention of the wild-type allele, when compared to untreated tumors (Figures 3A, 3B, and 3D). Treated and harvested *p53* mutant tumors (Figure S2C) exhibited heterogeneity in expression levels of several senescence markers, although only *Pml* was consistently elevated to a degree similar to that observed in *p53* wild-type tumors 5 days following treatment (Figure 3C). *Dcr2* was induced slightly following treatment in $p53^{R172H/0}$ tumors, possibly attributable to stromal cells within the tumor that still have the *p53* wild-type allele. We used orthotopic transplants of *p53* wild-type and mutant MMTV-*Wnt1*

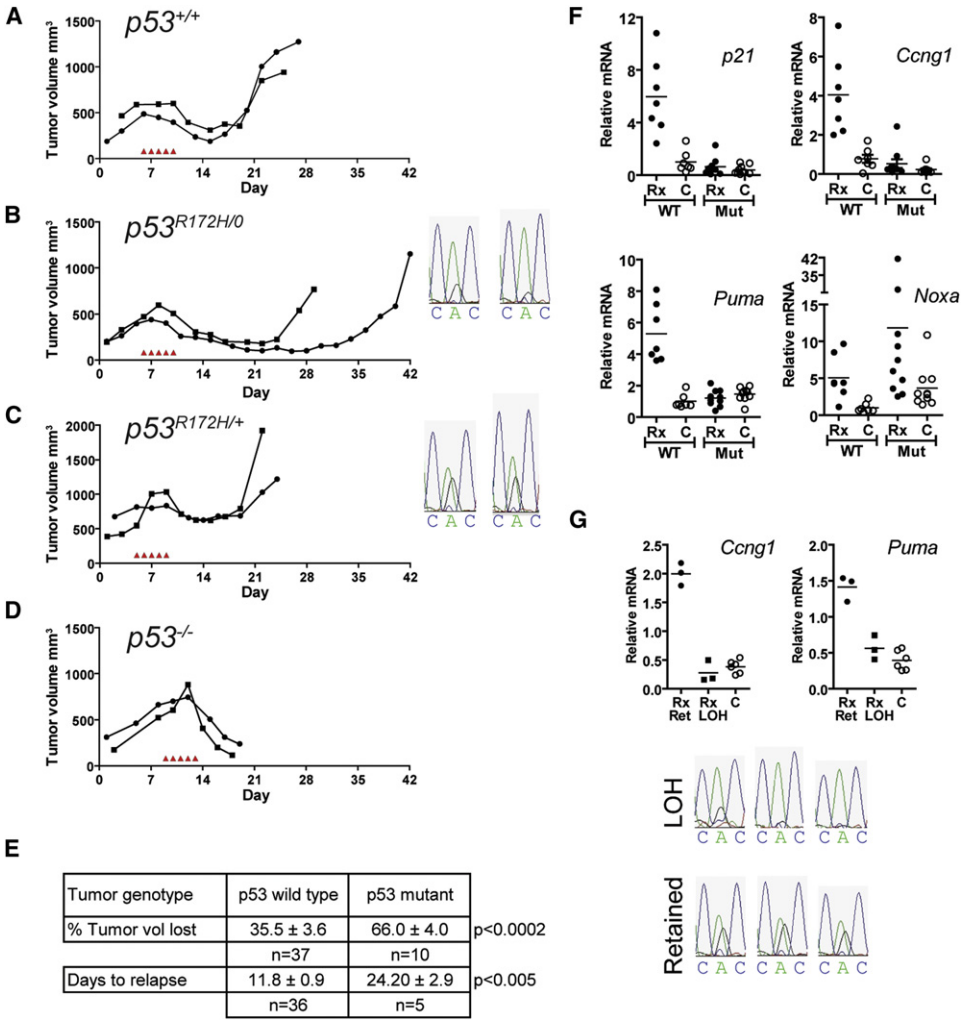

Tumor genotype	p53 wild type	p53 mutant	
% Tumor vol lost	35.5 ± 3.6	66.0 ± 4.0	p<0.0002
	n=37	n=10	
Days to relapse	11.8 ± 0.9	24.20 ± 2.9	p<0.005
	n=36	n=5	

Figure 1. Superior Response of *p53* Mutant MMTV-*Wnt1* Mammary Tumors to Doxorubicin Treatment

(A–D) MMTV-*Wnt1* mice bearing spontaneous, measurable, growing mammary tumors of approximately 500 mm^3 were injected once daily with 4 mg/kg doxorubicin for 5 consecutive days as indicated by arrowheads in graphs. Tumors with *p53* wild-type ($p53^{+/+}$) (A), heterozygous mutant that lost the wild-type allele ($p53^{R172H/0}$) (B), or retained the wild-type allele ($p53^{R172H/+}$) (C), and homozygous mutant ($p53^{-/-}$) (D) were measured regularly, and tumor volume was calculated. Shown are two representative mice for each genotype. LOH was determined by sequencing DNA from tumors across the region of the knockin point mutation. The double peak observed in (C) shows *p53* heterozygous status, whereas the single peak observed in (B) indicates LOH.

(E) Summary of responses for MMTV-*Wnt1* tumors with wild-type *p53* or $p53^{R172H/+}$ that retained the wild-type allele (n = 22 and n = 15, respectively, for tumor volume, total = 37; and n = 21 and n = 15, respectively, for relapse, total = 36) ("p53 wild-type") versus tumors homozygous mutant or $p53^{R172H/+}$ that underwent LOH (n = 2 and n = 8, respectively, for tumor volume, total = 10; and n = 1 and n = 4, respectively, for relapse, total = 5) ("p53 mutant"). Tumors showing primary resistance (~20%) were not included in analysis of response. Time to relapse is the number of days posttreatment by which tumor exceeded maximum tumor volume. Values shown are ± SEM.

(F) To measure *p53* activity, tumors were harvested 24 hr after the fifth and final doxorubicin injection ("Rx"), or from untreated control mice ("C") in *p53* wild-type (WT) or homozygous mutant (Mut) backgrounds. Relative mRNA levels determined by real-time RT-PCR are shown for indicated genes, with mean of WT C set to 1. Horizontal line is the mean.

(G) Tumors from $p53^{R172H/+}$ mice either retaining (Ret) or having lost (LOH) the wild-type allele were harvested 24 hr after the final doxorubicin treatment ("Rx") or from untreated control mice ("C"), and mRNA levels for indicated genes were determined as in (F). Horizontal line is the mean.

See also Figure S1.

tumors to further validate these findings. Parallel transplants of a *p53* wild-type tumor showed increased expression of senescence genes *p21* and *Dcr2* in cohorts that were treated and harvested 2 or 5 days following the final treatment compared to untreated or relapsed tumors, whereas induction of *Dec1* and *Pml* showed more variation among individual tumors (Figure 3E). A transplanted *p53* mutant tumor did not express markers of senescence following treatment at levels near the *p53* wild-type tumor, although a low-level induction of *p21* was observed, possibly attributable to *p53* wild-type stromal cells from the recipient (Figure 3F). We next examined senescence-associated β-galactosidase (SAβGal) staining in untreated versus treated MMTV-*Wnt1* tumor transplants. We found clearly positive SAβGal staining in gross tumor specimens from treated *p53*

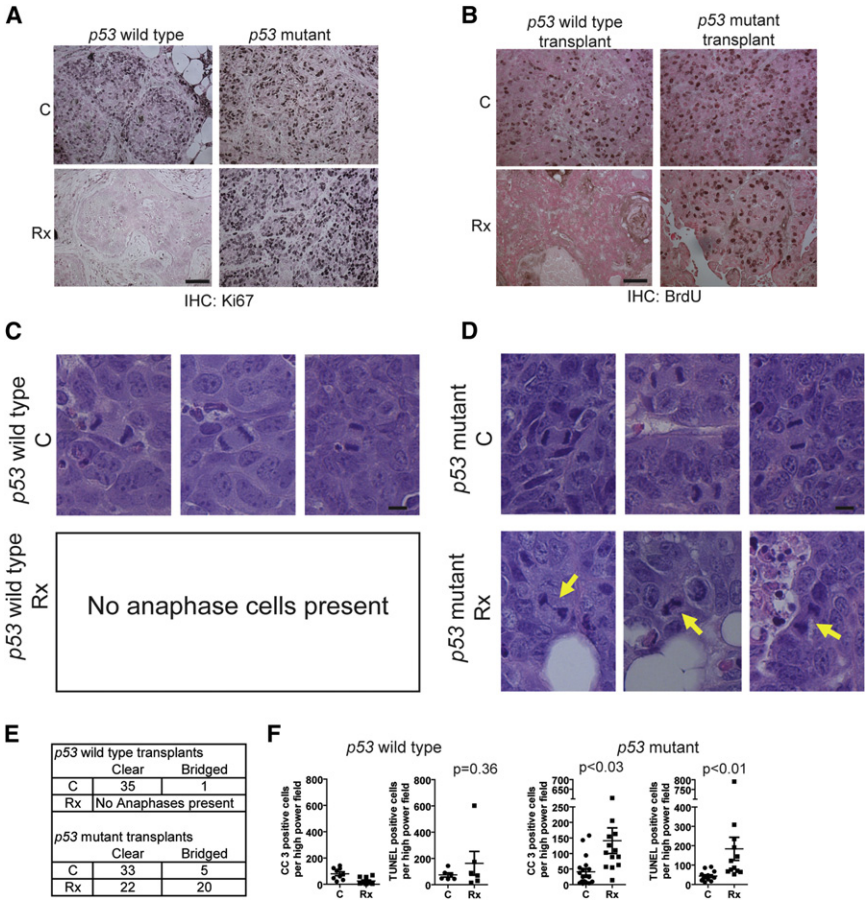

Figure 2. Failure to Arrest Leads to Aberrant Mitoses and Cell Death in Doxorubicin-Treated *p53* Mutant MMTV-*Wnt1* Tumors

(A) *p53* homozygous mutant and *p53* wild-type MMTV-*Wnt1* spontaneous tumors were harvested 24 hr following final treatment as in Figure 1F, and formalin-fixed, paraffin-embedded sections were stained for Ki67. Shown are representative images of five tumors from each group. Scale bar, 50 μM.

(B) An MMTV-*Wnt1* *p53* wild-type tumor and mutant ($p53^{R172H/0}$) tumor were harvested and processed to single-cell suspension by mincing and trypsinizing, and then 4×10^6 cells were injected into the abdominal mammary fat pads of recipient female C57BL6 mice. Tumors that formed were left untreated or given the usual five treatments of doxorubicin, followed by 2 BrdU injections 24 and 44 hr later, and then harvest 4 hr later (48 hr after final doxorubicin treatment). Formalin-fixed, paraffin-embedded sections were stained for BrdU. Scale bar, 50 μM.

(C and D) H&E sections from transplanted tumors in (B) were examined for anaphases and scored for bridges. Shown are three representative images from the *p53* wild-type tumor (C) and mutant ($p53^{R172H/0}$) tumor (D). Scale bars, 10 μM. Bridges are indicated by yellow arrows.

(E) Quantitation of anaphase bridges. "Clear" indicates no bridge observed.

(F) *p53* wild-type and *p53* homozygous mutant MMTV-*Wnt1* spontaneous tumors were harvested 24 hr following final treatment as in (A), and formalin-fixed, paraffin-embedded sections were stained for cleaved caspase-3 antibody or TUNEL as indicated in the figure. At least four random 200× high-powered fields per tumor were counted, averaged, and plotted, with mean ± SEM shown as line with error bars. The one *p53* wild-type tumor with a very high number of TUNEL-positive cells was also the only *p53* wild-type tumor that regressed during the treatment period (data not shown).

wild-type or $p53^{R172H/+}$ tumors, but not untreated tumors or transplanted $p53^{R172H/0}$ tumors that were treated (Figure S2D). Likewise, histological sections of only the treated *p53* wild-type or $p53^{R172H/+}$ tumors, but not $p53^{R172H/0}$ tumors, were positive for SAβGal (Figure 3G; data not shown). In sum we found that three out of three different *p53* wild-type tumors and three out of three different $p53^{R172H/+}$ tumor transplants were positive for SAβGal only after doxorubicin treatment, whereas histological sections of transplants from two different $p53^{R172H/0}$ tumors were negative, and gross specimens showed only faint staining in <10% of the tumor surface area. Together with the analysis of mRNA markers in Figures 3A–3C, our data show that transplanted and spontaneous tumors that retain a wild-type *p53* allele undergo cellular senescence following doxorubicin treatment.

The Role of *p21* in the Wild-type p53-Mediated Arrest Response to Doxorubicin

p21 is a major mediator of *p53*-dependent cell-cycle arrest and senescence and was strongly induced in the arrested *p53* wild-type tumors. Previous studies show that cells deficient for *p21* fail to arrest following DNA damage and fail to undergo senescence (Brown et al., 1997; Brugarolas et al., 1995; Bunz et al., 1998; Chang et al., 1999; Deng et al., 1995; Waldman et al., 1995), similar to the treated *p53* mutant MMTV-*Wnt1* tumors in this study. Thus, we hypothesized that *p21* null MMTV-*Wnt1* tumors would respond similarly to *p53* mutant tumors. To our surprise, we found that the *p21* null MMTV-*Wnt1* tumors exhibited on average a response intermediate between *p53* wild-type and mutant tumors (Figures 4A and S3A), with a significant subset showing a muted response similar to wild-type tumors (Figure 4A, upper chart) in addition to tumors that responded like *p53* mutant tumors (Figure 4A, lower chart). However, all *p21* null tumors examined were Ki67 positive (Figure 4B), suggesting that these tumors failed to arrest in G0. To further examine the *p21* null phenotypes, we used the amenable system of parallel orthotopic transplants of *p21* null MMTV-*Wnt1* tumors. We found examples of *p21* null MMTV-*Wnt1* tumors that arrested following treatment, ceased incorporating BrdU, and halted mitotic activity (transplant #1, Figure 4C), as well as *p21* null tumor transplants that failed to arrest, continued to incorporate BrdU, and underwent aberrant mitoses following treatment (Figures 4D, S3B, and S3C). In order to expand our examination of the arrest phenotype in *p21* null MMTV-*Wnt1*

tumors beyond these parallel transplants, we quantitated mitotic activity in ten spontaneous *p21* null MMTV-*Wnt1* tumors 24 hr following treatment to assess the fraction of these tumors that undergo arrest following treatment, compared to *p53* wild-type and mutant tumors. We found that six of ten tumors were essentially in mitotic arrest 24 hr following treatment, similar to five out of five *p53* wild-type-treated tumors (Figure 4E). However, mitotic activity persisted in four of ten treated tumors at a level similar to untreated tumors (Figure 4E). *p53* mutant MMTV-*Wnt1* tumors failed to arrest in all cases examined because mitotic figures were abundant in all eight treated spontaneous tumors. These data show that *p53* can mediate arrest in the absence of *p21* in a subset of tumors, providing a plausible explanation for the observation that some *p21* null tumors respond like *p53* wild-type tumors that arrest, and some like mutant tumors that fail to arrest.

The aforementioned results show that some *p21* null MMTV-*Wnt1* tumors arrested mitotic activity and cease incorporating BrdU after treatment, but all treated tumors examined were Ki67 positive (Figure 4B). This suggests that tumor cells were arrested somewhere in the cell cycle other than in G0. Indeed, FACS analysis revealed that orthotopic transplants of the BrdU-negative *p21* null tumor in Figure 4C arrested with 4n DNA content after treatment, consistent with a G2 arrest (Figure 5B), whereas the *p21/p53* wild-type transplanted MMTV-*Wnt1* tumor responded to treatment by a predominantly G1 arrest (Figure 5A). DNA content histograms of proliferating, relapsed tumors resembled those of proliferating untreated tumors (Figures 5A and 5B).

To address the mechanism of the G2 arrest in the two types of *p21* null responses, we examined G2 regulators. The *p21* null transplanted tumor that ceased DNA synthesis and mitosis (Figure 4C) had reduced levels of G2 regulators such as Cyclin B, Cdc2, and Stathmin1 (Figure 5C, upper chart, transplant #1). In contrast, *p21* null tumors that were BrdU positive after treatment and had aberrant mitoses (Figure 4D) failed to downregulate genes that promote transition through mitosis (Figure 5C, middle chart, transplant #2; Figure S4), similar to a transplanted *p53* mutant tumor (Figure 5C, lower chart). Thus, *p53*, in the absence of the cyclin-dependent kinase inhibitor *p21*, can still direct a G2 cell-cycle arrest in treated tumors, preventing the mitotic catastrophes associated with the superior response of *p53* mutant tumors. Although we were able to perform the extensive analysis using parallel orthotopic transplants of *p21* null tumors in only a limited number of tumors, our finding that even the *p21* null spontaneous tumors that lacked mitotic figures remained Ki67 positive suggests that these tumors likewise arrested outside of G0.

Senescence-Associated Cytokines Are Expressed in Doxorubicin-Treated Mammary Tumors

To further address the reason for early relapse in the arrested, senescent, *p53* wild-type MMTV-*Wnt1* tumors, we examined an array of cytokines and their receptors and cofactors that others have shown to be produced by normal cells made senescent after oncogenic stress (Acosta et al., 2008; Coppé et al., 2008; Kuilman et al., 2008; Wajapeyee et al., 2008). We found that our stably arrested, senescent MMTV-*Wnt1* tumors, either *p53* wild-type or heterozygous with retention of the wild-type allele (from Figures 3A and 3B), expressed elevated levels of a cytokine signaling network that included ligands and receptors (Figures 6A and 6B). Most tumors with mutant *p53* did not have significantly elevated levels of cytokines following treatment, with the exception of Rantes and Tnfα, although some approached significance (Figure 6C).

The senescent, cytokine-producing cells of the treated *p53* wild-type tumors did not undergo apoptosis, and the tumors did not lose significant volume as did *p53* mutant tumors (Figures 1 and 2). Therefore, we next tested whether the cytokines produced by the persistent senescent tumor cells could be detected in the sera of treated mice. Interestingly, we found no changes in serum levels of cytokines in treated *p53* wild-type mice with and without MMTV-*Wnt1* tumors at various stages before and following treatment (Figures S5A–S5D). This led us to test whether the expressed cytokines in treated tumors might be acting in a paracrine/autocrine manner. Stat transcription factors are activated by many of the cytokines elevated in treated, senescent, *p53* wild-type tumors and are important mediators of cytokine signaling (Clevenger, 2004; Novakova et al., 2010). Staining serial tumor sections, we found that untreated tumors were largely phospho-Stat3 negative, or showed only light nuclear staining, but were highly positive for the proliferation marker Ki67 (Figures S5E and S5F). Treated tumors, however, had regions of intense nuclear phospho-Stat3 staining that were Ki67 negative (Figures 6D, S5G, and S5H). Conversely, some regions in treated tumors were phospho-Stat3 negative, and Ki67 positive (Figure 6E). In fact many tumors had adjacent regions in the same field of view with this inverse phospho-Stat3/Ki67 staining (Figures 6F, 6G, S5I, and S5J). Interestingly, we also observed small areas within treated tumors that contained a mixed population of phospho-Stat3 and Ki67-positive cells along the borders of the inversely staining areas (Figure 6F, red outline; Figures S5K and S5L). This suggested the possibility that cytokines secreted by senescent cells could induce proliferation in neighboring, nonsenescent cells. Indeed, we found that Eotaxin and, to a lesser extent, Cxcl5 and Rantes could induce proliferation in cultured MMTV-*Wnt1* mammary tumor cells (Figure 6H, stimulation by known mitogens epidermal growth factor plus insulin is shown for comparison), suggesting a functional role for the cytokines produced by senescent cells in promoting tumor cell proliferation leading to clinical relapse.

To determine the role of *p21* in the induction of the senescence-associated cytokines, we examined treated, *p21* null MMTV-*Wnt1* tumors for expression of these genes. Treated spontaneous tumors did not show a clear induction of senescence markers, including cytokines and chemokines, when compared to untreated tumors (Figures S5M and S5N). It is possible that combining *p21* null MMTV-*Wnt1* tumors that arrest with those that continue proliferation following treatment could confound the interpretation of results in the spontaneous tumors. Therefore, we examined three parallel orthotopic transplants. We found that the *p21* null tumor that arrested following treatment (transplant #1) induced some senescent markers and cytokines following treatment (Figures S5O and S5P). Of the two tumors that failed to arrest following treatment, we found that one failed to induce any senescent markers or cytokines (Figures S5S and S5T), whereas the other strongly induced several

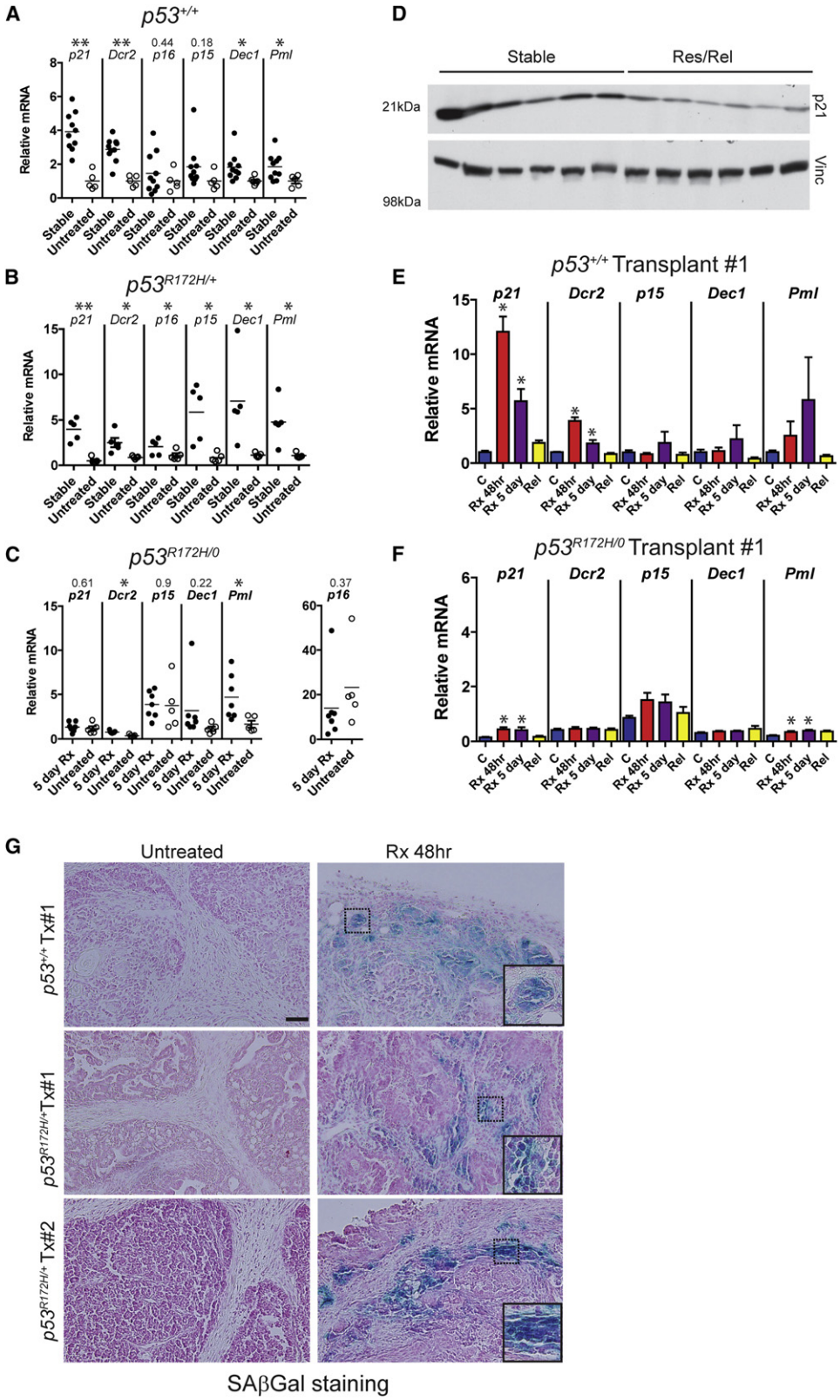

Figure 3. Wild-type *p53* Mediates Senescence following Doxorubicin Treatment of MMTV-*Wnt1* Tumors

(A–C) Spontaneous tumors were harvested from untreated mice or from mice 5–7 days following final doxorubicin treatment ("Stable"), and mRNA levels for senescence genes indicated in the figure were determined for *p53* wild-type MMTV-*Wnt1* tumors ($p53^{+/+}$) (A), *p53* heterozygous mutant tumors that retained the

senescence-associated cytokines (Figures S5Q and S5R). The fact that some treated *p21* null MMTV-*Wnt1* tumors retain the ability to induce senescence-associated cytokines following treatment could be a contributing factor in their early relapse.

Wild-type p53-Mediated Arrest Impairs Doxorubicin Response in Human Breast Cancer Cell Lines

We next investigated *p53-p21*-mediated response to doxorubicin in human breast cancer cells in culture. We found that MCF-7 and ZR-75.1 cells (*TP53* wild-type) treated with doxorubicin were positive for SAβGal activity, and induced cytokines following treatment that led to phosphorylation of STAT3 (Figures 7A–7C and S6A–S6C). Both cell lines also induced p53 and p21, ceased incorporating BrdU, and adopted a flattened morphology following doxorubicin treatment (Figures 7D–7F, S6D, and S6E), as previously described by Jackson and Pereira-Smith (2006). However, similar to the treated MMTV-*Wnt1* tumors lacking functional *p53*, MCF-7 and ZR-75.1 cells with *TP53* knockdown failed to arrest, adopted a rounded morphology consistent with cell death, and had fewer viable cells present following treatment than Si control-transfected, treated cells that adopted a senescent-like phenotype (Figures 7D–7G and S6D–S6F). Also consistent with our results in p53 wild-type and mutant MMTV-*Wnt1* tumors, both cell lines exhibited numerous aberrant mitoses, including anaphase bridges, and stark evidence of cell death such as micronuclei and condensed nuclei when treated after *TP53* or *p21* knockdown (Figures 7H and S6G). The response of MCF-7 and ZR-75.1 cells with *p21* knockdown was consistent with the subset of *p21* null MMTV-*Wnt1* tumors that continued to proliferate and enter mitosis following treatment. These data in breast cancer cell lines are similar to observations in other cell lines, such as the isogenic variants of the HCT-116 colon cancer cell line that lack *p53* or *p21* (Bunz et al., 1999; Waldman et al., 1997).

DISCUSSION

In this study we show that a robust response of breast cancer to chemotherapy is highly dependent on the absence of *p53*-mediated arrest. Functional *p53* activated a cell-cycle arrest/senescence program, preventing mitosis in the presence of DNA strand breaks. Treated tumors with mutant *p53* proceeded through the cell cycle and into aberrant mitoses. Another recent study observed that a *p53* mutant xenografted cell line showed an increase in aberrant mitotic figures after chemotherapy treatment, whereas a *p53* wild-type xenograft had increased SAβGal staining; however, outcome was not examined in this study (Varna et al., 2009).

Our data are consistent with retrospective human breast cancer studies showing that tumors with functional *p53* respond worse to dose-dense doxorubicin-based chemotherapy than tumors with nonfunctional *p53* (Bertheau et al., 2002, 2007). The delivery of a high dose of DNA-damaging agent is critical for this effect (Lehmann-Che et al., 2010). In addition to differing dose regimens used in conflicting studies, none of these reports stratified responses by LOH status of *TP53*. Our data presented here show that determining LOH status is critical for predicting response. We found that MMTV-*Wnt1* $p53^{R172H/+}$ tumors that retained the wild-type allele, despite the presence of the "dominant negative" point mutant (Lang et al., 2004; Willis et al., 2004), exhibited minimal tumor regression and had a transcriptional profile very similar to *p53* wild-type MMTV-*Wnt1* tumors, with acute expression of p53 targets and long-term expression of senescence markers. This finding has important clinical implications for using *TP53* status to risk stratify patients with breast cancer, where the wild-type allele is often retained (Mazars et al., 1992). Thus, identifying a *TP53* mutation without assessing LOH is a confounding factor likely responsible for the contradictory results observed in multiple studies analyzing the role of *TP53* mutational status in breast cancer response (Aas et al., 1996; Berns et al., 2000; Bertheau et al., 2002, 2007, 2008; Kröger et al., 2006; Makris et al., 1995; Mathieu et al., 1995). Furthermore, our results suggest that *TP53* mutations that occur in basal-like breast cancers contribute to the relatively high rate of complete responses observed in this subset (Carey et al., 2007; Straver et al., 2010) and also imply that these tumors are likely to undergo LOH. Conversely, in the luminal subtypes of breast cancer, which are mostly *TP53* wild-type, p53 activity could contribute to the lower frequency of complete remissions (Carey et al., 2007; Straver et al., 2010), and in instances where a *TP53* mutation is present in this subtype, the wild-type allele is likely to be retained. It will also be interesting to determine if the p53-mediated arrest phenotype we describe here is also predictive of poor chemotherapy response in other cancers.

Cells induced by doxorubicin to undergo senescence evidently persisted and likely contributed to the relapse. Our immunohistochemical analysis suggests that the cytokines secreted by senescent tumors operate in an autocrine or

wild-type allele ($p53^{R172H/+}$) (B), or lost the wild-type allele ($p53^{R172H/0}$) (C). p16 is shown on a separate axis due to the aberrantly high values in some tumors. All graphs in (A)–(C) are relative to the mean of untreated *p53* wild-type tumors set to a value of 1. For *p53* mutant tumors, responding tumors harvested 5 days after treatment (5 day Rx) (the time point when *p53* wild-type tumors express senescence markers) were used. $^{**}p < 0.005$; $^{*}p < 0.05$ by Student's t test; p values of nonsignificant comparisons are shown above the gene symbol. Horizontal line is the mean.

(D) *p21* protein levels in six of the tumors from (A) compared to growing, relapsed tumors as determined by western blot, with Vinculin (Vinc) used as a control. Student's t test of densitometric analysis of the two groups, $p = 0.0045$.

(E and F) Parallel transplanted tumors as in Figure 2B were untreated ("C") or doxorubicin treated ("Rx") and harvested 48 hr or 5 days after the final treatment, or followed until relapse ("Rel"). mRNA levels for senescence genes indicated in the figure were determined for *p53* wild-type (E) and mutant (F) transplanted tumors, in at least four tumors for each treatment group. Values in mutant tumors in (F) are relative to untreated tumors in (E) and shown on a smaller scale so differences can be discerned. $^{*}p < 0.05$ by ANOVA and Newman-Keuls posttest for comparison to untreated. Error bars are ± SEM.

(G) SAβGal staining in histological sections of untreated and treated orthotopic tumor transplants. Shown are representative sections from one *p53* wild-type donor and two different $p53^{R172H/+}$ donors, with and without doxorubicin treatment. Similar results were observed in a total of three out of three wild-type and three out of three $p53^{R172H/+}$-transplanted tumors. Insets shown in bottom-right corner are higher-magnification images of the area shown outlined in black within the image. Scale bar, 50 μM.

See also Figure S2.

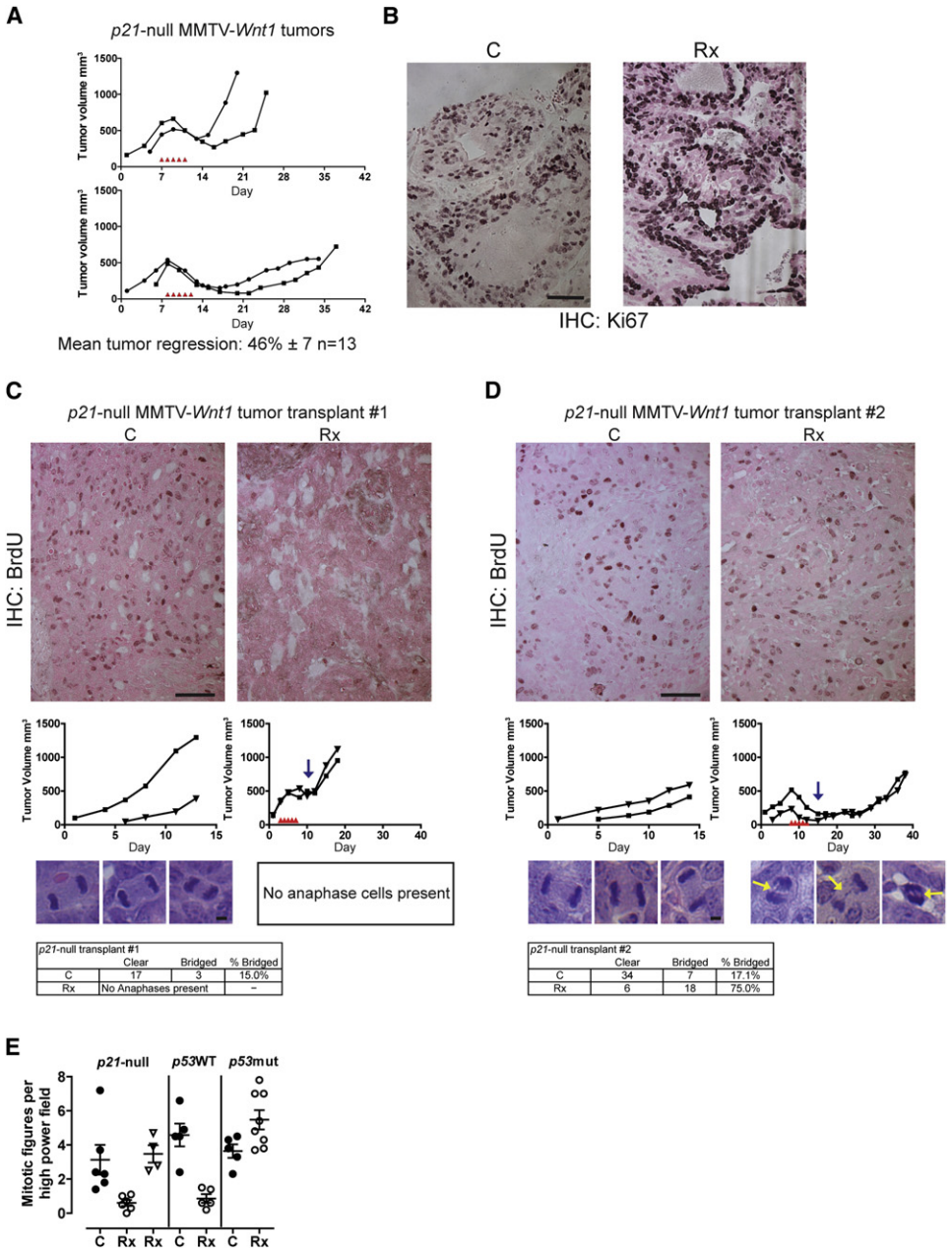

Figure 4. Dichotomous Responses in Doxorubicin-Treated *p21* null MMTV-*Wnt1* Mice: Subsets of Tumors Retain Arrest Capability, whereas Others Continue Proliferation

(A) *p21* null MMTV-*Wnt1* mice bearing spontaneous, measurable, growing mammary tumors of approximately 500 mm^3 were injected once daily with 4 mg/kg doxorubicin for 5 consecutive days as indicated by red arrowheads in graphs. Shown are representative charts from mice with poor (top) and favorable (bottom) responses, and mean tumor regression ± SEM.

(B) Ki67 IHC staining of untreated ("C") and treated ("Rx") *p21* null MMTV-*Wnt1* tumors harvested 24 hr following the final treatment is presented. Shown are representative images from seven treated and six untreated or relapsed tumors. Scale bar, 50 μM.

(C and D) Two different *p21* null MMTV-*Wnt1* tumors were transplanted, treated in parallel, and BrdU incorporation was determined as in Figure 2B. Shown are representative images of BrdU staining (scale bar, 50 μM), the corresponding tumor volume charts for parallel transplanted tumors that were followed (blue arrow indicates the 48 hr time point when parallel transplants were harvested for analysis), representative anaphases (scale bar, 5 μM), and a table quantitating the anaphase data.

(E) H&E sections from untreated ("C") and treated ("Rx") tumors of the indicated genotypes were quantitated for mitotic figures. Each data point represents the average count of mitotic figures in ten 400× high-power field views. *p21* null MMTV-*Wnt1*-treated tumors were separated into arrested (open circles) and mitotic (open triangles) groups. Mean (horizontal line) with error bars (SEM) is shown.

See also Figure S3.

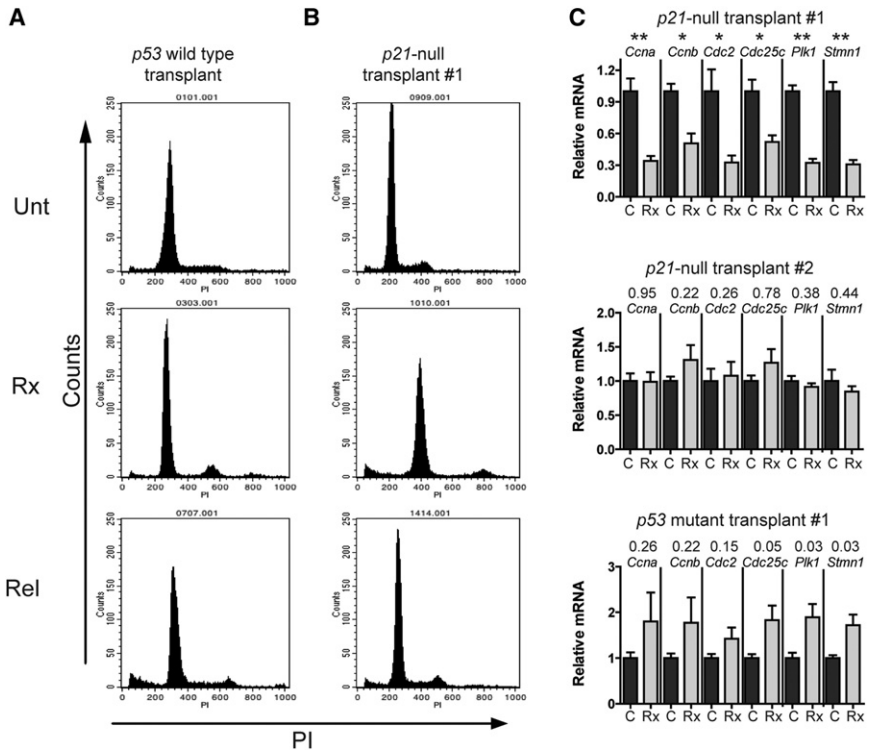

Figure 5. G2 Arrest with Downregulated G2-M Regulators in Nonproliferating *p21* Null MMTV-*Wnt1*-Treated Tumors

(A and B) *p53* wild-type and *p21* null MMTV-*Wnt1* tumors were transplanted and treated in parallel as in Figure 2B and harvested. Tumors as indicated in the figure were processed to single-cell suspension by mincing and trypsinizing, followed by fixation and staining for DNA content with propidium iodide (PI). Unt, untreated; Rx, doxorubicin treated; Rel, relapsed.

(C) mRNA levels for G2-M regulatory genes as indicated in the figure were determined for untreated tumors ("C") or tumors harvested 48 hr after final treatment ("Rx"); at least three tumors were analyzed per treatment group. Error bars are ± SEM. $^{**}p < 0.005$, $^{*}p < 0.05$ by Student's t test. p Values of nonsignificant comparisons and comparisons where treated tumors were higher are shown above the gene symbol.

See also Figure S4.

paracrine fashion, reinforcing the dormant state (Kuilman et al., 2008). However, we also found Ki67 and phospho-Stat3 double-positive regions in treated tumors that were nearing the time at which they typically relapse. Because cytokines promote the proliferation of nonsenescent mammary tumor cells, this suggests that neighboring, nonsenescent cells within the tumor could be stimulated to proliferate by cytokines produced by senescent cells. Of note the cytokines we tested for growth stimulation represent just three of many potentially mitogenic cytokines expressed in the senescent tumor cells. Also, it is not known what additive or synergistic growth effects the array of cytokines expressed by tumor cells would have within the natural environment of the tumor. Indeed, others have shown various cytokines elevated in our tumors to have protumorigenic properties in different cellular contexts (Begley et al., 2008; Dhawan and Richmond, 2002; Pirianov and Colston, 2001; Takamori et al., 2000; Yang et al., 2006). Furthermore, it is also possible that the cytokines promote other phenotypes such as metastasis and cell survival (Clevenger, 2004; Karnoub and Weinberg, 2006-2007; Krtolica et al., 2001). The finding that some *p53* mutant tumors also expressed selected cytokines following treatment underscores the importance of apoptosis in these tumors. Apoptosis likely eliminated the damaged *p53* mutant tumor cells that expressed mitogenic cytokines, whereas cytokine producing cells in a *p53* wild-type tumor persisted in a senescent state.

Our work also suggests that pharmacological inhibition of arrest and/or senescence, by inactivating *p53*, could improve chemotherapy response by redirecting cells toward apoptosis. However, it is important to note that complete loss of *p21* in the MMTV-*Wnt1* tumors was insufficient to bypass the *p53*-mediated arrest phenotype in a subset of tumors. *p21* null MMTV-*Wnt1* tumors showed a dichotomy of responses, resulting in an intermediate mean tumor regression following treatment. This is consistent with these tumors having both a "*p53* wild-type like" response, where treated tumors do not enter S phase or mitosis, arresting in G2, and a "*p53* mutant-like" response, where treated tumors continued through S phase and mitosis. This effect has not been observed in several in vitro studies of a *p21* null cell line. Using isogenic variants of the colon cancer cell line HCT-116, Waldman et al. observed a superior response to radiation in *p21* null xenografts, as compared to the parental cell line (Waldman et al., 1997). These data, from a single xenografted cell line, are consistent with the fraction of tumors in our study that failed to arrest following treatment (Waldman et al., 1997).

In summary we have modeled chemotherapy response in mice, showing that p53 activity induces *p21*-dependent and -independent growth arrest and cellular senescence instead of cell death, resulting in minimal tumor regression and early relapse. Bypassing senescence, via *p53* deletion/mutation, initiated *p53*-independent cell death and improved tumor response. These results provide a compelling explanation for previous studies that showed improved patient response to anthracycline-based chemotherapy in *TP53* mutant human breast tumors (Bertheau et al., 2002, 2007).

EXPERIMENTAL PROCEDURES

Mice

All experiments were approved by the MD Anderson Cancer Center Institutional Animal Care and Use Committee, Protocol ID# 079906634, and conformed to the guidelines of the United States Animal Welfare Act and the National Institutes of Health. MMTV-*Wnt1*, $p53^{R172H/R172H}$, $p53^{-/-}$, and $p21^{-/-}$ mice have been described by Brugarolas et al. (1995), Jacks et al. (1994), Lang et al. (2004), and Tsukamoto et al. (1988). Breeders were backcrossed into C57Bl6J background (The Jackson Laboratory, Bar Harbor, ME, USA) until >90% C57Bl6J as determined by polymorphic allele analysis

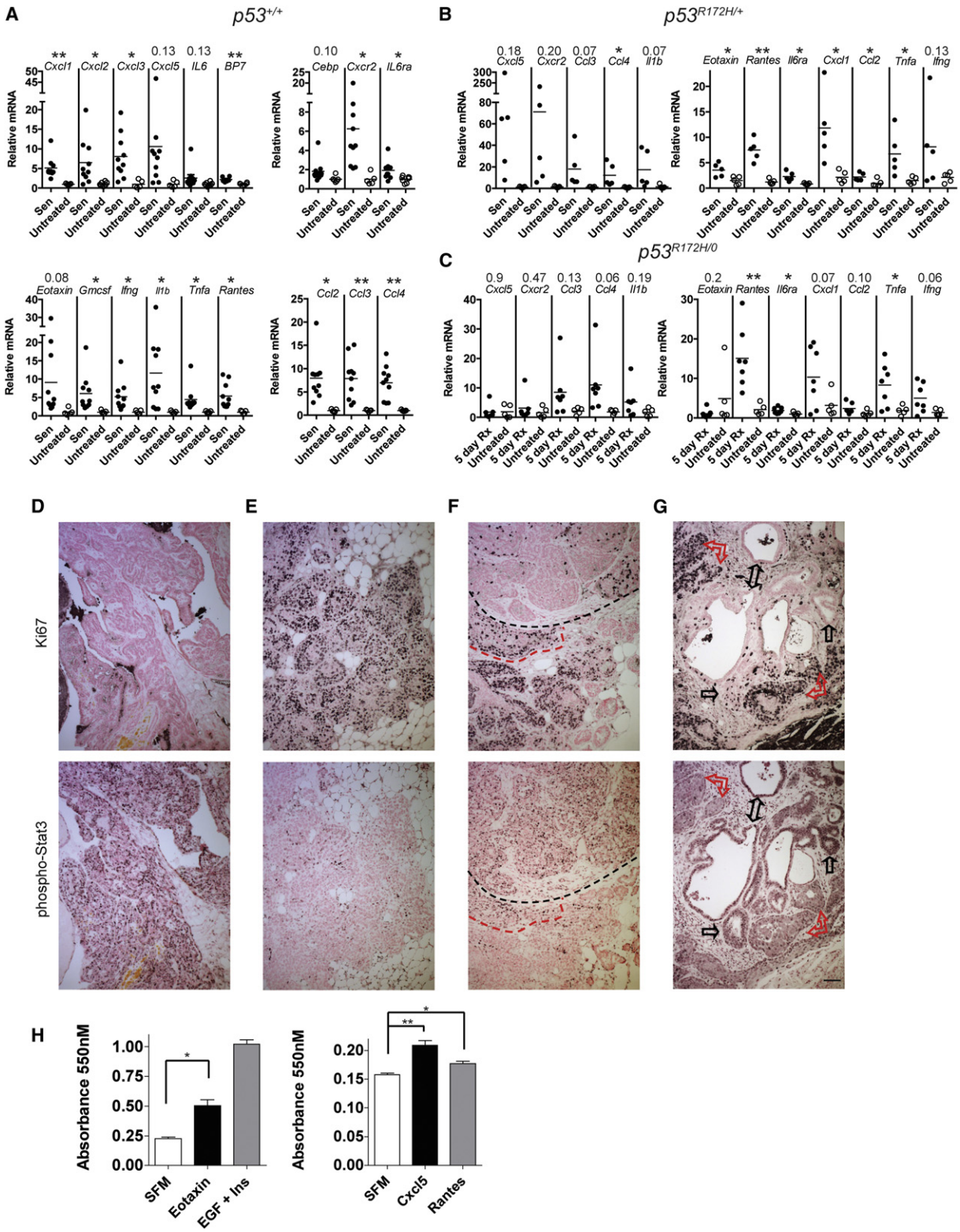

Figure 6. Senescence-Associated Cytokines Are Expressed in Treated MMTV-*Wnt1* Mammary Tumors

(A–C) *p53* wild-type tumors (A), *p53* heterozygous mutant tumors that retained the wild-type allele (B), or lost the wild-type allele (C), corresponding to spontaneous tumors from Figures 3A–3C, were harvested, and mRNA levels for genes indicated in the figure were determined. All graphs in (A)–(C) are relative to the mean of untreated *p53* wild-type tumors set to a value of 1. $^{**}p < 0.005$, $^{*}p < 0.05$ by Student's t test. p Values of nonsignificant comparisons are shown above the gene symbol. Horizontal line is the mean.

by the Research Animal Support Facility-Smithville, Genetic Services. Subsequent breedings produced MMTV-*Wnt1* mice in *p53* wild-type, $p53^{R172H/R172H}$, $p53^{-/-}$, $p53^{R172H/+}$, and $p21^{-/-}$ backgrounds. Homozygous *p53* mutant mice, particularly females, were not born at Mendelian ratio, consistent with other reports by Sah et al. (1995), and were thus difficult to acquire in the cohort. Mammary tumors formed in MMTV-*Wnt1* mice in our study with median latency of 185 days. $p53^{R172H/R172H}$, $p53^{-/-}$ and $p53^{R172H/+}$ mice had median latencies of 108, 111, and 173 days, respectively. Mice were monitored frequently for tumor formation and tumors measured regularly using digital calipers: tumor volume in mm^3 = (width^2 × length)/2 (Bearss et al., 2000). Histologically, all of the MMTV-*Wnt1* tumors were ductal carcinomas, generally of solid, cystic, or mixed subtypes. *p53* wild-type, $p53^{R172H/+}$, $p21^{-/-}$ were all 68%–79% mixed, whereas $p53^{R172H/R172H}$ and $p53^{R172H/0}$ were 61% solid. When tumors reached a volume of ~500 mm^3 and were growing, 4 mg/kg doxorubicin (Sigma-Aldrich, St. Louis) in PBS was injected intraperitoneally once daily for 5 consecutive days. Treatments were well tolerated in *p53* wild-type and heterozygous mutant mice as well as $p21^{-/-}$ mice, with minimal (less than 10%) or no weight loss during or after treatment. *p53* homozygous mutant mice, however, did show signs of toxicity, primarily weight loss ~4 days after treatment, likely due to GI syndrome, as previously described in *p53* mutant mice by Komarova et al. (2004). This toxicity did not appear to contribute to tumor regression because *p53* heterozygous mutant mice with LOH in the tumor had no toxicity and had similar tumor regression as the homozygous mutant mice. At the defined endpoint for each mouse, tumors were harvested, and portions were fixed in formalin for 48 hr and paraffin embedded (FFPE), and also flash frozen for biochemical analysis. LOH analysis was performed exactly as previously described by Post et al. (2010).

Real-Time RT-PCR

RNA was extracted from frozen, pulverized tumors using TRIzol reagent (Invitrogen, Carlsbad, CA, USA), subjected to DNase treatment (Roche, Indianapolis, IN, USA), and then reverse transcribed using a kit (GE Healthcare, Piscataway, NJ, USA). Real-time PCR using Sybr green (BioRad, Valencia, CA, USA) was performed as previously described by Jackson and Pereira-Smith (2006). Expression was normalized to Gapdh and verified with Rplp0. Primer sequences are available on request.

Immunohistochemistry

Cleaved caspase staining was performed as previously described by Post et al. (2010), and staining for phospho-Stat3 polyclonal antibody (1:100; Cell Signaling, Danvers, MA, USA) and Ki67 (1:100; Leica, Newcastle Upon Tyne, UK, Ki67-MM1) were performed similarly. For phospho-Stat3 monoclonal, antigen retrieval was in Tris EDTA buffer (pH 9). For detecting incorporation of BrdU, tumor-bearing mice were injected with BrdU (Invitrogen) according to manufacturer's instructions, 24 and 4 hr before harvest, followed by standard fixation and processing. Denaturation was in 2 N HCl for 90 min, followed by neutralization in 0.1 M $Na_2B_4O_7$, standard processing, and then incubation with anti-BrdU (BD Immunocytometry Systems, San Jose, CA, USA) at 1:40 for 1 hr (McGinley et al., 2000). Antigen detection for immunohistochemistry (IHC) was performed using a VECTASTAIN kit and ABC (Vector Laboratories, Burlingame, CA, USA). Images were acquired on a Nikon 80i microscope equipped with a Nikon DS-Fi1 color camera using the 10×/0.45 objective and Nikon Elements software. Some images were processed minimally in Adobe Photoshop only by histogram stretching and gamma adjustment. At least four random fields were manually counted for cleaved caspase-3 experiments. Number of positive cells was averaged for the four fields.

TUNEL staining was performed using the FragEL DNA fragmentation detection kit (Calbiochem, Darmstadt, Germany) and quantitated as above. SAβGal assay was performed essentially as described by Dimri et al. (1995) for in vitro and in vivo experiments. Tumor segments ~1 mm thick were fixed in 2% formaldehyde, 0.2% glutaraldehyde in PBS, stained for SAβGal, cut to 6 μm sections, and counterstained with Nuclear Fast Red (Vector Laboratories). These results were verified by staining of frozen sections in parallel.

Western Blotting

Frozen pulverized tumors were lysed and separated by SDS-PAGE as previously described by Pant et al. (2011). Antibodies and dilutions were p21 (for mouse p21 detection), 1:1,000, #556431 (BD PharMingen, San Jose, CA, USA); Vinculin, 1:1,000, #V-9131 (Sigma-Aldrich); p21 (for human p21 detection), 1:200, SC6246 (Santa Cruz Biotechnology, Santa Cruz, CA, USA); and mouse monoclonal p53, 1:200, OP09 (EMD Biosciences, Darmstadt, Germany).

Statistical Analysis

Two-tailed Student's t tests and ANOVA using Newman-Keuls posttest were performed using GraphPad Prism software (La Jolla, CA, USA).

Anaphase Bridges and Mitotic Activity

H&E MMTV-*Wnt1* tumor sections were scanned on a microscope at 400×, and cells in anaphase were photographed. Two different observers identified the presence or absence of bridges. For mitotic figures, ten random, 400×, high-powered fields for each tumor were selected, and mitotic figures were identified and counted by two different observers.

Flow Cytometry

Tumors were harvested and processed as for transplants (above). After filtering, cells were washed in PBS, then fixed in 70% ethanol for at least 24 hr at −20°C. Propidium iodide staining was performed as previously described by Jackson and Pereira-Smith (2006).

Transplants

Primary MMTV-*Wnt1* tumors were removed from euthanized mice, minced thoroughly with a scalpel blade, and then trypsinized for 10 min at 37°C. Trypsin was inactivated with DMEM plus 10% fetal calf serum, followed by passage through a 40 μM filter. After PBS washing, cells were resuspended in Matrigel/PBS (BD Biosciences) at a concentration of 4 × 10^6/50 μl. The 50 μl solution was injected into each abdominal mammary fat pad of recipient C57Bl6 mice using a 30G needle. Tumors were detectable at ~2 weeks, typically.

SUPPLEMENTAL INFORMATION

Supplemental Information includes six figures and Supplemental Experimental Procedures and can be found with this article online at doi:10.1016/j.ccr.2012.04.027.

ACKNOWLEDGMENTS

The authors wish to thank MDACC Animal Support Facility-Smithville, the DNA Analysis Facility, the Flow Cytometry & Imaging Core Facility, and the

(D–G) Phospho-Stat3 and Ki67 staining in treated, senescent tumors. Serial sections from formalin-fixed paraffin-embedded tumors from Figure 3A were stained for Ki67 (upper panels) or phosphoTyr705-Stat3 (antibody clone D3A7) (lower panels). (D–F) Representative examples of positive/negative or negative/positive phospho-Stat3 (antibody clone D3A7) and Ki67 from treated tumors. (F) Inverse staining of adjacent areas within the same tumor sections, and an area of double positivity marked by red dashed line. (G) Similar staining results with a second polyclonal phosphoTyr705-Stat3 antibody, with more intense phospho-Stat3-positive/Ki67-negative areas (indicated by black arrows) and less intense phospho-Stat3 staining/Ki67-positive areas (indicated by red arrows). Scale bar, 50 μM. (H) Tumor cells isolated from an MMTV-*Wnt1* mammary tumor and cultured were plated at 8,000 cells per well in a 24-well plate overnight, then media were changed to serum-free media (SFM), or 100 ng/ml cytokine. EGF and insulin, known mitogens in breast cancer, were at 20 ng/ml and 10 μg/ml, respectively. Cell number was determined at day 4 by MTT assay. Error bars are ± SEM. For comparison of SFM to Eotaxin, *$p < 0.05$ by Student's t test. For comparison of SFM, Cxcl5, and Rantes, $p < 0.005$ by ANOVA and Newman-Keuls.
See also Figure S5.

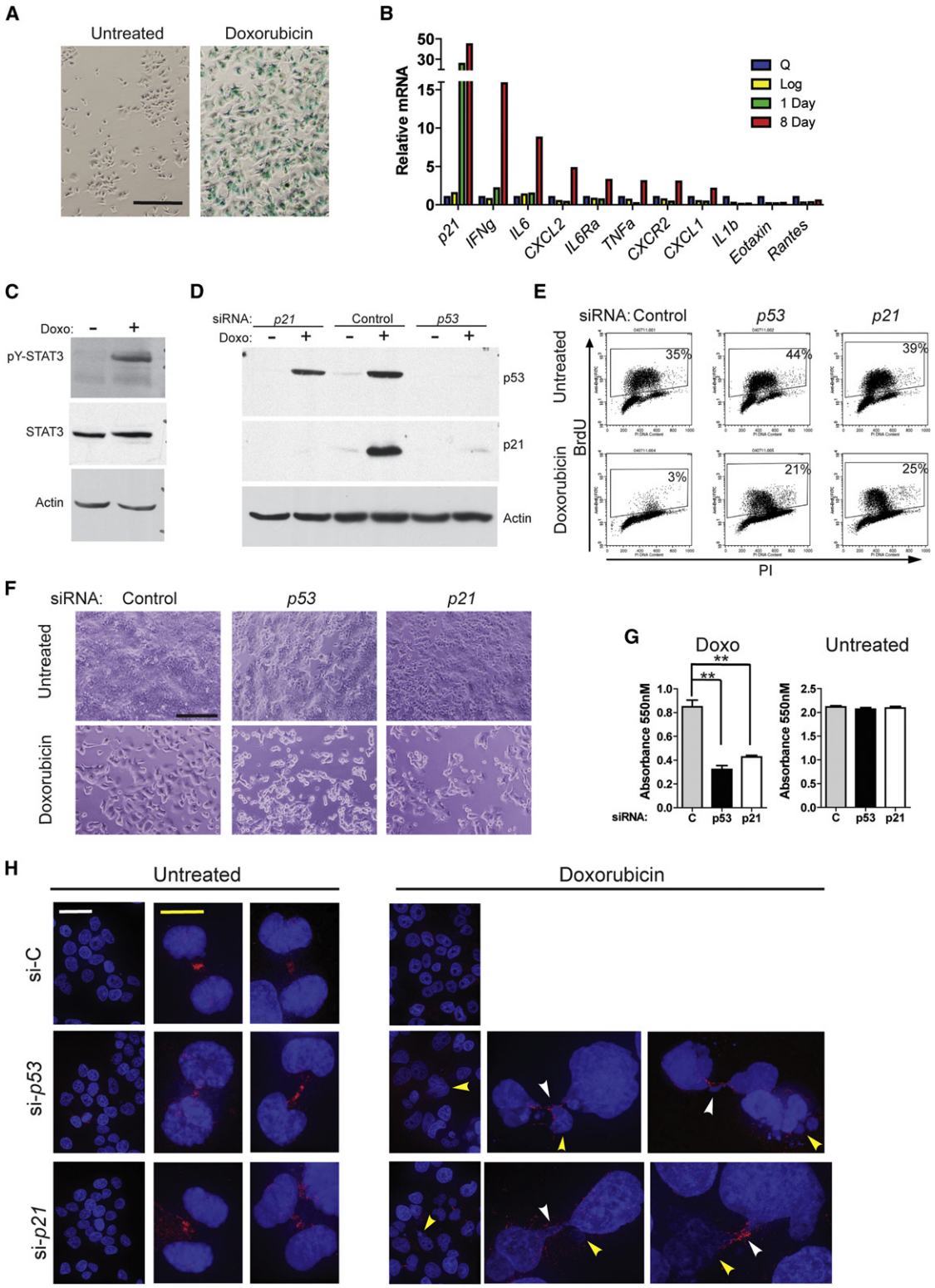

Figure 7. *p53* or *p21* Knockdown Improves Doxorubicin Response in *p53* Wild-type MCF-7 Breast Cancer Cells

(A) MCF-7 human breast cancer cells untreated or treated with 200 nM doxorubicin for 24 hr and harvested 8 days later were fixed and stained for SAβGal. Scale bar, 500 μM.

(B) mRNA levels for cytokines indicated in the figure were determined for MCF-7 cells that were serum starved for 72 hr (Q), growing in log phase (Log), or treated with doxorubicin as in (A) and harvested 1 or 8 days later.

Department of Veterinary Medicine and Surgery and the Histology Core Research Lab, each supported by NCI Grant CA16672. We also acknowledge Courtney Vallien for histological sectioning, Henry P. Adams for technical help with microscopy, and Archana Sidalaghatta Nagaraja for assistance with mouse necropsy and RNA preparation. J.G.J. was funded as an Odyssey Scholar by the Theodore N. Law Endowment for Scientific Achievement, a Dodie P. Hawn Fellowship in Genetics, and by NIH Grant U01DE019765-01. Q.L. and V.P. are supported by NIH Grant CA47296. G.L. is supported by NIH Grants CA34936 and CA82577.

J.G.J. conceived, designed, and performed all the experiments except where noted, and wrote the manuscript. V.P. and J.G.J. performed protein expression analysis. J.G.J., Q.L., and V.P. performed mRNA analysis. J.G.J., L.L.C., Q.L., D.G., and A.Q.-C. performed immunohistochemical analyses. T.M. performed the Bio-Plex cytokine array. J.G.J., D.G., and A.Q.-C. performed quantitative analysis of mitosis. Y.L. developed cell lines. J.G.J. and O.T. performed senescence associated β-galactosidase studies. P.Y. and J.G.J. determined loss of heterozygosity in tumors. A.K.E-N. performed pathological analysis. A.Q.-C. edited the manuscript. G.L. was the principal investigator for the study.

Received: October 1, 2011
Revised: March 2, 2012
Accepted: April 14, 2012
Published: June 11, 2012

REFERENCES

Aas, T., Børresen, A.L., Geisler, S., Smith-Sørensen, B., Johnsen, H., Varhaug, J.E., Akslen, L.A., and Lønning, P.E. (1996). Specific P53 mutations are associated with de novo resistance to doxorubicin in breast cancer patients. Nat. Med. *2*, 811–814.

Acosta, J.C., O'Loghlen, A., Banito, A., Guijarro, M.V., Augert, A., Raguz, S., Fumagalli, M., Da Costa, M., Brown, C., Popov, N., et al. (2008). Chemokine signaling via the CXCR2 receptor reinforces senescence. Cell *133*, 1006–1018.

Bearss, D.J., Subler, M.A., Hundley, J.E., Troyer, D.A., Salinas, R.A., and Windle, J.J. (2000). Genetic determinants of response to chemotherapy in transgenic mouse mammary and salivary tumors. Oncogene *19*, 1114–1122.

Begley, L.A., Kasina, S., Mehra, R., Adsule, S., Admon, A.J., Lonigro, R.J., Chinnaiyan, A.M., and Macoska, J.A. (2008). CXCL5 promotes prostate cancer progression. Neoplasia *10*, 244–254.

Berns, E.M., Foekens, J.A., Vossen, R., Look, M.P., Devilee, P., Henzen-Logmans, S.C., van Staveren, I.L., van Putten, W.L., Inganäs, M., Meijer-van Gelder, M.E., et al. (2000). Complete sequencing of TP53 predicts poor response to systemic therapy of advanced breast cancer. Cancer Res. *60*, 2155–2162.

Bertheau, P., Plassa, F., Espié, M., Turpin, E., de Roquancourt, A., Marty, M., Lerebours, F., Beuzard, Y., Janin, A., and de Thé, H. (2002). Effect of mutated TP53 on response of advanced breast cancers to high-dose chemotherapy. Lancet *360*, 852–854.

Bertheau, P., Turpin, E., Rickman, D.S., Espié, M., de Reyniès, A., Feugeas, J.P., Plassa, L.F., Soliman, H., Varna, M., de Roquancourt, A., et al. (2007). Exquisite sensitivity of TP53 mutant and basal breast cancers to a dose-dense epirubicin-cyclophosphamide regimen. PLoS Med. *4*, e90.

Bertheau, P., Espié, M., Turpin, E., Lehmann, J., Plassa, L.F., Varna, M., Janin, A., and de Thé, H. (2008). TP53 status and response to chemotherapy in breast cancer. Pathobiology *75*, 132–139.

Bonnefoi, H., Piccart, M., Bogaerts, J., Mauriac, L., Fumoleau, P., Brain, E., Petit, T., Rouanet, P., Jassem, J., Blot, E., et al; EORTC 10994/BIG 1-00 Study Investigators. (2011). TP53 status for prediction of sensitivity to taxane versus non-taxane neoadjuvant chemotherapy in breast cancer (EORTC 10994/BIG 1-00): a randomised phase 3 trial. Lancet Oncol. *12*, 527–539.

Brown, J.M., and Attardi, L.D. (2005). The role of apoptosis in cancer development and treatment response. Nat. Rev. Cancer *5*, 231–237.

Brown, J.P., Wei, W., and Sedivy, J.M. (1997). Bypass of senescence after disruption of p21CIP1/WAF1 gene in normal diploid human fibroblasts. Science *277*, 831–834.

Brugarolas, J., Chandrasekaran, C., Gordon, J.I., Beach, D., Jacks, T., and Hannon, G.J. (1995). Radiation-induced cell cycle arrest compromised by p21 deficiency. Nature *377*, 552–557.

Bunz, F., Dutriaux, A., Lengauer, C., Waldman, T., Zhou, S., Brown, J.P., Sedivy, J.M., Kinzler, K.W., and Vogelstein, B. (1998). Requirement for p53 and p21 to sustain G2 arrest after DNA damage. Science *282*, 1497–1501.

Bunz, F., Hwang, P.M., Torrance, C., Waldman, T., Zhang, Y., Dillehay, L., Williams, J., Lengauer, C., Kinzler, K.W., and Vogelstein, B. (1999). Disruption of p53 in human cancer cells alters the responses to therapeutic agents. J. Clin. Invest. *104*, 263–269.

Carey, L.A., Dees, E.C., Sawyer, L., Gatti, L., Moore, D.T., Collichio, F., Ollila, D.W., Sartor, C.I., Graham, M.L., and Perou, C.M. (2007). The triple negative paradox: primary tumor chemosensitivity of breast cancer subtypes. Clin. Cancer Res. *13*, 2329–2334.

Chang, B.D., Xuan, Y., Broude, E.V., Zhu, H., Schott, B., Fang, J., and Roninson, I.B. (1999). Role of p53 and p21waf1/cip1 in senescence-like terminal proliferation arrest induced in human tumor cells by chemotherapeutic drugs. Oncogene *18*, 4808–4818.

Clarke, A.R., Purdie, C.A., Harrison, D.J., Morris, R.G., Bird, C.C., Hooper, M.L., and Wyllie, A.H. (1993). Thymocyte apoptosis induced by p53-dependent and independent pathways. Nature *362*, 849–852.

Clevenger, C.V. (2004). Roles and regulation of stat family transcription factors in human breast cancer. Am. J. Pathol. *165*, 1449–1460.

Collado, M., Gil, J., Efeyan, A., Guerra, C., Schuhmacher, A.J., Barradas, M., Benguría, A., Zaballos, A., Flores, J.M., Barbacid, M., et al. (2005). Tumour biology: senescence in premalignant tumours. Nature *436*, 642.

Coppé, J.P., Patil, C.K., Rodier, F., Sun, Y., Muñoz, D.P., Goldstein, J., Nelson, P.S., Desprez, P.Y., and Campisi, J. (2008). Senescence-associated secretory phenotypes reveal cell-nonautonomous functions of oncogenic RAS and the p53 tumor suppressor. PLoS Biol. *6*, 2853–2868.

Deng, C., Zhang, P., Harper, J.W., Elledge, S.J., and Leder, P. (1995). Mice lacking p21CIP1/WAF1 undergo normal development, but are defective in G1 checkpoint control. Cell *82*, 675–684.

Dhawan, P., and Richmond, A. (2002). Role of CXCL1 in tumorigenesis of melanoma. J. Leukoc. Biol. *72*, 9–18.

Dimri, G.P., Lee, X., Basile, G., Acosta, M., Scott, G., Roskelley, C., Medrano, E.E., Linskens, M., Rubelj, I., Pereira-Smith, O., et al. (1995). A biomarker that identifies senescent human cells in culture and in aging skin in vivo. Proc. Natl. Acad. Sci. USA *92*, 9363–9367.

(C) MCF-7 cells untreated or 8 days following treatment as in (A) were harvested 48 hr after a media change, and western blots were performed with indicated antibodies.
(D–F) MCF-7 cells were transfected with nontargeting siRNA (Control) or siRNA targeting *p53* or *p21*. After 24 hr, cells were treated with doxorubicin for 24 hr, or untreated as indicated. (D) Cells were harvested 24 hr after treatment for western blot with *p53*, *p21*, or actin antibodies. (E) Cells were pulsed for 1 hr with BrdU 24 hr after doxorubicin treatment, fixed, stained with anti-BrdU FITC, and sorted by flow cytometry. Percent BrdU-positive cells are indicated in the figure. (F) Four days following treatment and media change, cells were photographed using bright-field microscopy (scale bar, 500 μM).
(G) Cell number was determined by MTT assay 9 days following treatment. Error bars are ± SEM. $^{**}p < 0.005$ by ANOVA and Newman-Keuls posttest.
(H) MCF-7 cells were untreated or treated with 200 nM doxorubicin for 24 hr, then fixed and stained for α-tubulin and DAPI 72 hr later. Scale bars, 40 μM (white) and 10 μM (yellow). Yellow arrows indicate micronuclei and white arrows anaphase bridges.
See also Figure S6.

Donehower, L.A., Godley, L.A., Aldaz, C.M., Pyle, R., Shi, Y.P., Pinkel, D., Gray, J., Bradley, A., Medina, D., and Varmus, H.E. (1995). Deficiency of p53 accelerates mammary tumorigenesis in Wnt-1 transgenic mice and promotes chromosomal instability. Genes Dev. *9*, 882–895.

Jacks, T., Remington, L., Williams, B.O., Schmitt, E.M., Halachmi, S., Bronson, R.T., and Weinberg, R.A. (1994). Tumor spectrum analysis in p53-mutant mice. Curr. Biol. *4*, 1–7.

Jackson, J.G., and Pereira-Smith, O.M. (2006). Primary and compensatory roles for RB family members at cell cycle gene promoters that are deacetylated and downregulated in doxorubicin-induced senescence of breast cancer cells. Mol. Cell. Biol. *26*, 2501–2510.

Jackson, J.G., Post, S.M., and Lozano, G. (2011). Regulation of tissue- and stimulus-specific cell fate decisions by p53 in vivo. J. Pathol. *223*, 127–136.

Karnoub, A.E., and Weinberg, R.A. (2006–2007). Chemokine networks and breast cancer metastasis. Breast Dis. *26*, 75–85.

Komarova, E.A., Kondratov, R.V., Wang, K., Christov, K., Golovkina, T.V., Goldblum, J.R., and Gudkov, A.V. (2004). Dual effect of p53 on radiation sensitivity in vivo: p53 promotes hematopoietic injury, but protects from gastrointestinal syndrome in mice. Oncogene *23*, 3265–3271.

Kröger, N., Milde-Langosch, K., Riethdorf, S., Schmoor, C., Schumacher, M., Zander, A.R., and Löning, T. (2006). Prognostic and predictive effects of immunohistochemical factors in high-risk primary breast cancer patients. Clin. Cancer Res. *12*, 159–168.

Krtolica, A., Parrinello, S., Lockett, S., Desprez, P.Y., and Campisi, J. (2001). Senescent fibroblasts promote epithelial cell growth and tumorigenesis: a link between cancer and aging. Proc. Natl. Acad. Sci. USA *98*, 12072–12077.

Kuilman, T., Michaloglou, C., Vredeveld, L.C., Douma, S., van Doorn, R., Desmet, C.J., Aarden, L.A., Mooi, W.J., and Peeper, D.S. (2008). Oncogene-induced senescence relayed by an interleukin-dependent inflammatory network. Cell *133*, 1019–1031.

Lang, G.A., Iwakuma, T., Suh, Y.A., Liu, G., Rao, V.A., Parant, J.M., Valentin-Vega, Y.A., Terzian, T., Caldwell, L.C., Strong, L.C., et al. (2004). Gain of function of a p53 hot spot mutation in a mouse model of Li-Fraumeni syndrome. Cell *119*, 861–872.

Lehmann-Che, J., André, F., Desmedt, C., Mazouni, C., Giacchetti, S., Turpin, E., Espié, M., Plassa, L.F., Marty, M., Bertheau, P., et al. (2010). Cyclophosphamide dose intensification may circumvent anthracycline resistance of p53 mutant breast cancers. Oncologist *15*, 246–252.

Liu, G., Parant, J.M., Lang, G., Chau, P., Chavez-Reyes, A., El-Naggar, A.K., Multani, A., Chang, S., and Lozano, G. (2004). Chromosome stability, in the absence of apoptosis, is critical for suppression of tumorigenesis in Trp53 mutant mice. Nat. Genet. *36*, 63–68.

Lowe, S.W., Ruley, H.E., Jacks, T., and Housman, D.E. (1993a). p53-dependent apoptosis modulates the cytotoxicity of anticancer agents. Cell *74*, 957–967.

Lowe, S.W., Schmitt, E.M., Smith, S.W., Osborne, B.A., and Jacks, T. (1993b). p53 is required for radiation-induced apoptosis in mouse thymocytes. Nature *362*, 847–849.

Lowe, S.W., Bodis, S., McClatchey, A., Remington, L., Ruley, H.E., Fisher, D.E., Housman, D.E., and Jacks, T. (1994). p53 status and the efficacy of cancer therapy in vivo. Science *266*, 807–810.

Makris, A., Powles, T.J., Dowsett, M., and Allred, C. (1995). p53 protein overexpression and chemosensitivity in breast cancer. Lancet *345*, 1181–1182.

Mathieu, M.C., Koscielny, S., Le Bihan, M.L., Spielmann, M., and Arriagada, R.; Institut Gustave-Roussy Breast Cancer Group. (1995). p53 protein overexpression and chemosensitivity in breast cancer. Lancet *345*, 1182.

Mazars, R., Spinardi, L., BenCheikh, M., Simony-Lafontaine, J., Jeanteur, P., and Theillet, C. (1992). p53 mutations occur in aggressive breast cancer. Cancer Res. *52*, 3918–3923.

McGinley, J.N., Knott, K.K., and Thompson, H.J. (2000). Effect of fixation and epitope retrieval on BrdU indices in mammary carcinomas. J. Histochem. Cytochem. *48*, 355–362.

Novakova, Z., Hubackova, S., Kosar, M., Janderova-Rossmeislova, L., Dobrovolna, J., Vasicova, P., Vancurova, M., Horejsi, Z., Hozak, P., Bartek, J., and Hodny, Z. (2010). Cytokine expression and signaling in drug-induced cellular senescence. Oncogene *29*, 273–284.

Pant, V., Xiong, S., Iwakuma, T., Quintás-Cardama, A., and Lozano, G. (2011). Heterodimerization of Mdm2 and Mdm4 is critical for regulating p53 activity during embryogenesis but dispensable for p53 and Mdm2 stability. Proc. Natl. Acad. Sci. USA *108*, 11995–12000.

Pirianov, G., and Colston, K.W. (2001). Interactions of vitamin D analogue CB1093, TNFalpha and ceramide on breast cancer cell apoptosis. Mol. Cell. Endocrinol. *172*, 69–78.

Post, S.M., Quintás-Cardama, A., Terzian, T., Smith, C., Eischen, C.M., and Lozano, G. (2010). p53-dependent senescence delays Emu-myc-induced B-cell lymphomagenesis. Oncogene *29*, 1260–1269.

Rahko, E., Blanco, G., Soini, Y., Bloigu, R., and Jukkola, A. (2003). A mutant TP53 gene status is associated with a poor prognosis and anthracycline-resistance in breast cancer patients. Eur. J. Cancer *39*, 447–453.

Riley, T., Sontag, E., Chen, P., and Levine, A. (2008). Transcriptional control of human p53-regulated genes. Nat. Rev. Mol. Cell Biol. *9*, 402–412.

Sah, V.P., Attardi, L.D., Mulligan, G.J., Williams, B.O., Bronson, R.T., and Jacks, T. (1995). A subset of p53-deficient embryos exhibit exencephaly. Nat. Genet. *10*, 175–180.

Soussi, T., and Lozano, G. (2005). p53 mutation heterogeneity in cancer. Biochem. Biophys. Res. Commun. *331*, 834–842.

Straver, M.E., Glas, A.M., Hannemann, J., Wesseling, J., van de Vijver, M.J., Rutgers, E.J., Vrancken Peeters, M.J., van Tinteren, H., Van't Veer, L.J., and Rodenhuis, S. (2010). The 70-gene signature as a response predictor for neoadjuvant chemotherapy in breast cancer. Breast Cancer Res. Treat. *119*, 551–558.

Takamori, H., Oades, Z.G., Hoch, O.C., Burger, M., and Schraufstatter, I.U. (2000). Autocrine growth effect of IL-8 and GROalpha on a human pancreatic cancer cell line, Capan-1. Pancreas *21*, 52–56.

te Poele, R.H., Okorokov, A.L., Jardine, L., Cummings, J., and Joel, S.P. (2002). DNA damage is able to induce senescence in tumor cells in vitro and in vivo. Cancer Res. *62*, 1876–1883.

Tsukamoto, A.S., Grosschedl, R., Guzman, R.C., Parslow, T., and Varmus, H.E. (1988). Expression of the int-1 gene in transgenic mice is associated with mammary gland hyperplasia and adenocarcinomas in male and female mice. Cell *55*, 619–625.

Varna, M., Lehmann-Che, J., Turpin, E., Marangoni, E., El-Bouchtaoui, M., Jeanne, M., Grigoriu, C., Ratajczak, P., Leboeuf, C., Plassa, L.F., et al. (2009). p53 dependent cell-cycle arrest triggered by chemotherapy in xenografted breast tumors. Int. J. Cancer *124*, 991–997.

Wajapeyee, N., Serra, R.W., Zhu, X., Mahalingam, M., and Green, M.R. (2008). Oncogenic BRAF induces senescence and apoptosis through pathways mediated by the secreted protein IGFBP7. Cell *132*, 363–374.

Waldman, T., Kinzler, K.W., and Vogelstein, B. (1995). p21 is necessary for the p53-mediated G1 arrest in human cancer cells. Cancer Res. *55*, 5187–5190.

Waldman, T., Zhang, Y., Dillehay, L., Yu, J., Kinzler, K., Vogelstein, B., and Williams, J. (1997). Cell-cycle arrest versus cell death in cancer therapy. Nat. Med. *3*, 1034–1036.

Willis, A., Jung, E.J., Wakefield, T., and Chen, X. (2004). Mutant p53 exerts a dominant negative effect by preventing wild-type p53 from binding to the promoter of its target genes. Oncogene *23*, 2330–2338.

Yang, X., Lu, P., Fujii, C., Nakamoto, Y., Gao, J.L., Kaneko, S., Murphy, P.M., and Mukaida, N. (2006). Essential contribution of a chemokine, CCL3, and its receptor, CCR1, to hepatocellular carcinoma progression. Int. J. Cancer *118*, 1869–1876.